

Investigation of Electrical Modulus Behavior in $\text{LiNi}_{3/5}\text{Fe}_{2/5}\text{VO}_4$ Ceramics

Moti Ram

Department of Physics and Meteorology, Indian Institute of Technology, Kharagpur, West Bengal-721302, India

Abstract: The ceramics ($\text{LiNi}_{3/5}\text{Fe}_{2/5}\text{VO}_4$) was prepared by solution-based chemical method and it has an orthorhombic unit cell structure with lattice parameters $a = 3.78 \text{ \AA}$, $b = 15.82 \text{ \AA}$ and $c = 5.56 \text{ \AA}$. Complex electrical modulus result shows: single-phase character of the material in good agreement with the observations made from X-ray diffraction, and non-Debye type (polydisperse) conductivity relaxation in the ceramics. The value of activation energy was determined from the Arrhenius plot of relaxation time vs. $10^3/\text{Temperature}$ as $\sim (0.157 \pm 0.003) \text{ eV}$ at $21\text{-}100 \text{ }^\circ\text{C}$.

Keywords: Ceramics; Chemical preparation, Complex electrical modulus; Conductivity relaxation, Relaxation time.

1. Introduction

Recently, scientists and industry peoples have given great attention to lithiated transition metal oxides because of their physical properties and technological applications [1, 2]. The concept of electrical modulus is associated with ionic/electronic conductivity in such oxides under the influence of a.c. field [3, 4]. Our study is concerned with frequency and temperature dependence of electrical modulus properties and associated conductivity relaxation phenomena of lithiated transition metal oxides. Electrical modulus presents an alternative approach based on polarization analysis [5, 6]. Complex electrical modulus plots give more importance to elements with the smallest capacitance occurring in the dielectric system. The electrical modulus $M^*(\omega)$ as expressed in the complex modulus formalisms are: $M^*(\omega) = 1/\epsilon^* = j(\omega C_0)Z^* = M' + jM''$, $M' = \omega C_0 Z''$ and $M'' = \omega C_0 Z'$, where (M', Z') and (M'', Z'') are real and imaginary part of electrical modulus and impedance respectively, $j = (-1)^{1/2}$, $\omega =$ angular frequency ($2\pi f$) and C_0 (geometrical capacitance) = $\epsilon_0 A/t$ (where $\epsilon_0 =$ permittivity for free space, $A =$ area of the electrode surface and $t =$ thickness) [7, 8]. In the present investigation, a systematic study on electrical modulus properties of the system ($\text{LiNi}_{3/5}\text{Fe}_{2/5}\text{VO}_4$) has been undertaken. Electrical modulus properties of $\text{LiNi}_{3/5}\text{Fe}_{2/5}\text{VO}_4$ were studied using complex impedance spectroscopy method.

2. Experimental Procedures

Solution-based chemical method was used to synthesize the $\text{LiNi}_{3/5}\text{Fe}_{2/5}\text{VO}_4$ system. The stoichiometric amounts of highly pure LiNO_3 (98%, M/s Loba Chemie Pvt. Ltd., India), $\text{Ni}(\text{NO}_3)_2 \cdot 6\text{H}_2\text{O}$ (98%, E. Merck (India) Ltd.), $\text{Fe}(\text{NO}_3)_3 \cdot 9\text{H}_2\text{O}$ ($\geq 98\%$, E. Merck (India) Ltd.) and NH_4VO_3 (99%, M/s s.d. fine-chem Pvt. Ltd., India) were dissolved in distilled water and mixed together. Thereafter triethanolamine ($>97\%$, E. Merck (India) Ltd.) was added maintaining a ratio of 3:1 with metal ions. HNO_3 (68-72%, E. Merck (India) Ltd.) and oxalic acid ($>99\%$, E. Merck (India) Ltd.) were added to dissolve the precipitate and then the clear solution was evaporated at $\sim 200 \text{ }^\circ\text{C}$ temperature with continuous stirring. A fluffy, mesoporous and carbon-rich precursor mass was formed by complete evaporation of the

solution. After grinding, the voluminous, fluffy and black carbonaceous mass was calcined at $525 \text{ }^\circ\text{C}$ for 4 h to produce the desired phase, which was confirmed by X-ray diffraction analysis. The calcined powder was cold pressed into circular disc shaped pellet of diameter 12-13 mm and various thicknesses with polyvinyl alcohol as the binder using hydraulic press at a pressure of $\sim 7.85\text{-}9.81 \text{ MPa}$. These pellets were then sintered at $575 \text{ }^\circ\text{C}$ for 2 h followed by slow cooling process. The heating and cooling rates during calcination and sintering processes were $3 \text{ }^\circ\text{C} / \text{min}$. The binder was removed during the sintering process. Subsequently, the pellets were polished by fine emery paper to make their faces smooth and parallel. One such sintered pellet of average thickness (1.52 mm) and radius (5.59 mm) was taken for electrical measurements. This pellet was finally coated with conductive silver paint and dried at $150 \text{ }^\circ\text{C}$ for 3 h before carrying out electrical measurements. Electrical modulus measurements were measured by applying a voltage of $\sim 0.701 \text{ V}$ using a computer-controlled frequency response analyzer (HIOKI LCR Hi TESTER, Model: 3532-50) with varying temperature over the frequency range of $10^2\text{-}10^6 \text{ Hz}$.

3. Results and Discussion

The $\text{LiNi}_{3/5}\text{Fe}_{2/5}\text{VO}_4$ has an orthorhombic unit cell structure with lattice parameters ($a = 3.78 \text{ \AA}$, $b = 15.82 \text{ \AA}$ and $c = 5.56 \text{ \AA}$) and polycrystalline texture with grains of different sizes $\sim 0.1\text{-}2.0 \text{ }\mu\text{m}$, which are revealed by X-ray diffraction and field emission scanning electron microscopy analysis, respectively [9]. Furthermore, X-ray diffraction observation shows that the material under consideration has single phase [9].

Complex modulus spectrums (M' vs. M'') at different temperatures are shown in Fig. 1. It confirms: (i) asymmetric semicircular arcs in the pattern which suggests the existence of electrical relaxation phenomena in the material, and (ii) single phase character of the material in good agreement with the observations made from X-ray diffraction [10, 5].

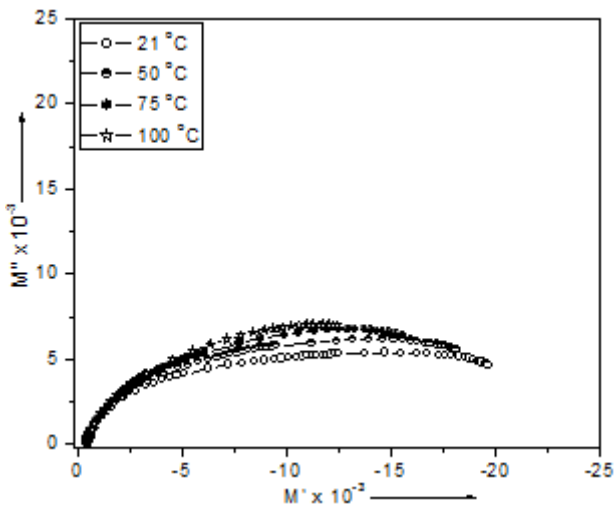


Figure 1: Complex modulus spectrum of $\text{LiNi}_{3/5}\text{Fe}_{2/5}\text{VO}_4$ at different temperatures.

Variation of M' as a function of frequency at different temperatures is presented in Fig. 2. It is clear that, M' reaches a maximum constant value $M_\infty = 1/\epsilon_\infty$ at higher frequencies and approaches zero at low frequencies. These characteristics indicate that the electrode polarization makes a negligible contribution in the material, and dispersion causes conductivity relaxation [11]. Furthermore, M' levels off at higher frequencies and temperatures due to the spread of relaxation processes over a range of frequencies [11, 5].

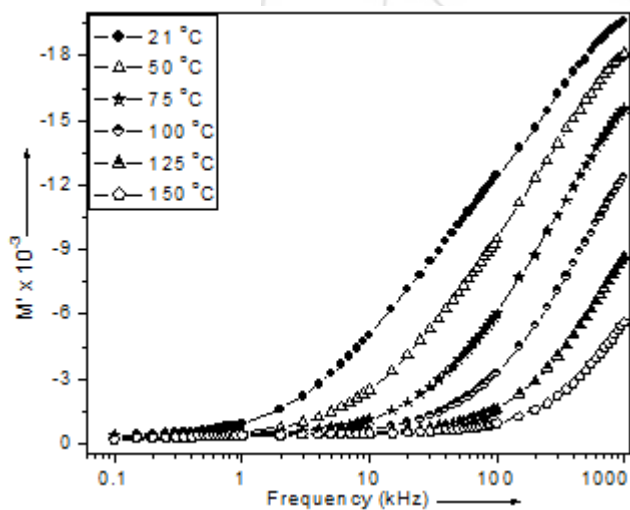


Figure 2: Variation of M' as a function of frequency at different temperatures.

Fig. 3 indicates the variation of M'' with frequency at different temperatures. It is seen from the figure that M'' increases as frequency rises and takes a peak value at a particular frequency [i.e., relaxation frequency (f_r)]. It is proportional to d.c. conductivity and indicates the presence of conductivity relaxation in the material [12, 13]. The frequency regions to the left and right of peak indicate the range in which charge carriers are mobile on long and short distance, respectively. Shifting of the peaks towards the higher frequency side with increasing temperature shows temperature dependence of conductivity relaxation time $\tau_\sigma (=$

$1/2\pi f_r$). Moreover, the asymmetrical broadening of the peaks indicates relaxation being non-Debye type [14-16, 8].

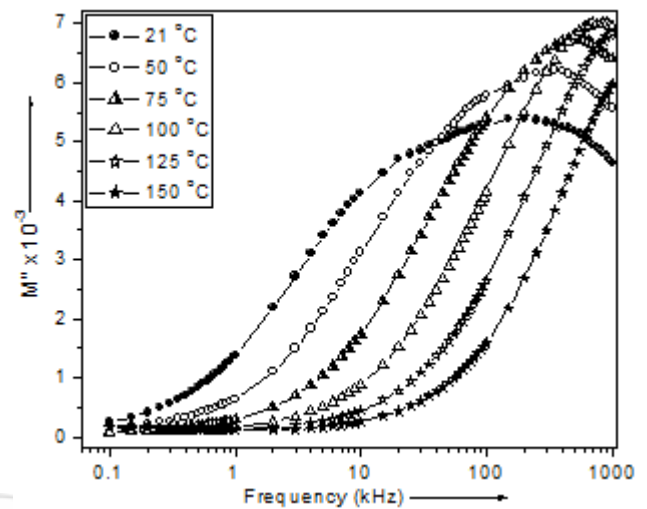


Figure 3: Variation of M'' as a function of frequency at different temperatures

The variation of τ_σ as a function of temperature is shown in Fig. 4. The decreasing nature of τ_σ with temperature indicates that relaxation mechanism is a thermally activated process. This variation obeys the Arrhenius relation [$\tau_\sigma = \tau_{\sigma 0} \exp(-E_a/kT)$], where $\tau_{\sigma 0}$ is the pre-exponential factor, E_a is activation energy, k is Boltzmann constant, and T is the absolute temperature [17, 18]. The value of E_a has been calculated using the Arrhenius relation and slope of the plot as $\sim (0.157 \pm 0.003)$ eV at 21-100 °C.

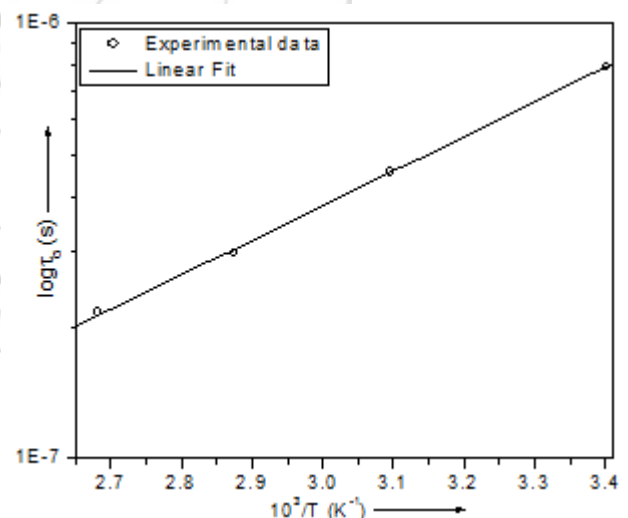


Figure 4: Variation of relaxation time (τ_σ) as a function of temperature.

The variation of M''/M''_{\max} with $\log(f/f_{\max})$ at different temperatures (Fig. 5) indicates the scaling behavior in the sample. Approximately, same shape and pattern with slight variation in FWHM (≥ 1.14 decade) with increasing temperature has been observed. In the pattern, low frequency

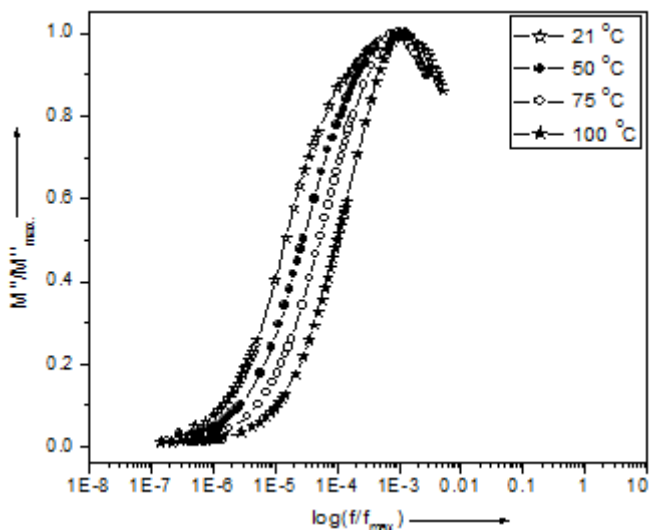


Figure 5: The variation of $M''/M''_{max.}$ with $\log(f/f_{max.})$ at different temperatures

region of the peak is denominated by d.c. conductivity, and a slight dispersion is observed in the high frequency region [19]. This behavior suggests that the dynamical processes occurring within the sample at different frequencies exhibit the same thermal activation energy and are independent of temperature with non-Debye type of conductivity relaxation. Furthermore, this pattern suggests that the movement of ions takes place via hopping mechanism [20, 16].

4. Conclusions

The $\text{LiNi}_{3/5}\text{Fe}_{2/5}\text{VO}_4$ system has orthorhombic unit cell structure with lattice parameters ($a = 3.78 \text{ \AA}$, $b = 15.82 \text{ \AA}$ and $c = 5.56 \text{ \AA}$) and polycrystalline texture with grains of unequal sizes $\sim 0.1\text{-}2.0 \text{ \mu m}$. This system has been produced by solution-based chemical method. A detailed electrical modulus study indicates that conductivity relaxation in the material is non-Debye type (polydispersive) and thermally activated process. The activation energy calculated from electrical modulus spectra is $\sim (0.157 \pm 0.003) \text{ eV}$ at 21-100 °C.

5. Acknowledgements

The author is grateful to the Nanomaterials Laboratory of the Department of Chemistry and Central Research Facility, Indian Institute of Technology, Kharagpur-721302 (W.B.), India, for providing facilities to conduct experiments.

References

[1] G. Lorenzi, G. Baldi, D. F. Benedetto, V. Faso, P. Lattanzi, and M. Romanelli, "Spectroscopic study of a Ni-bearing gahnite pigment", *Journal of the European Ceramic Society*, vol. 26, no.3, pp. 317-321, 2006.
 [2] A. L. Fernández, and L. Pablo, "Formation and the color development in cobalt spinel pigments", *Pigment and Resin Technology*, vol. 31, no.6, pp. 350-356, 2002.
 [3] K. Iwachi, "Dielectric properties of fine particles of Fe_3O_4 and some ferrites", *Japanese Journal of Applied Physics*, vol. 10, no. 11, pp. 1520-1528, 1971.

[4] A. M. M. Farea, S. Kumar, K. M. Batoo, A. Yousef, C. G. Lee, and Alimuddin, "Structure and electrical properties of $\text{Co}_{0.5}\text{Cd}_x\text{Fe}_{2.5-x}\text{O}_4$ ferrites", *Journal of Alloys and Compounds.*, vol. 464, no.1-2, pp. 361-369, 2008.
 [5] J. R. MacDonald, "Impedance Spectroscopy: Emphasizing Solid Materials and Systems", John Wiley & Sons, New York, 1987.
 [6] P. B. Macedo, C. T. Moynihan, and R. Bose, "Role of ionic diffusion in polarization in vitreous ionic conductors", *Physics and Chemistry of Glasses*, vol. 13, no.6, pp. 171-179, 1972.
 [7] S. Sen, P. Pramanic, and R. N. P. Choudhary, "Impedance spectroscopy study of the nanocrystalline ferroelectric $(\text{PbMg})(\text{ZrTi})\text{O}_3$ system", *Applied Physics A-Materials Science and Processing*, vol. 82, no.3, pp. 549-557, 2006.
 [8] J. M. Reau, A. Simon, M. E. Omari, and J. Ravez, "Impedance spectroscopy analysis of $\text{Pb}_5\text{Al}_3\text{F}_{19}$ ", *Journal of the European ceramic Society*, vol. 19, no. 6-7, pp. 777-779, 1999.
 [9] M. Ram, "Frequency and temperature-dependent electrical properties of $\text{LiNi}_{3/5}\text{Fe}_{2/5}\text{VO}_4$ studied by complex impedance spectroscopy", *Journal of Physics and Chemistry of Solids*, vol. 73, no.1, pp. 25-29, 2012.
 [10] N. G. McCrum, B. E. Read, and G. Williams, "Anelastic and Dielectric Effects in Polymeric Solids", Wiley, New York, 1967.
 [11] B. V. R. Chowdari, and R. Gopalkrishnan, "ac conductivity analysis of glassy silver iodomolybdate system". *Solid State Ionics*, vol. 23, no.3, pp. 225-233, 1987.
 [12] A. Molak, M. Paluch, S. Pawlus, Z. Ujma, M. Pawelczyk, and I. Gruszka, "Properties of $(\text{Bi}_{1/9}\text{Na}_{2/3})(\text{Mn}_{1/3}\text{Nb}_{2/3})\text{O}_3$ analysed within dielectric permittivity, conductivity, electric modulus and derivative techniques approach", *Phase Transitions: A Multinational Journal*, vol. 79, no.6-7, pp. 447-460, 2006.
 [13] A. Kumar, B. P. Singh, R. N. P. Choudhary, and A. K. Thakur, "A.C. impedance analysis of the effect of dopant concentration on electrical properties of calcium modified BaSnO_3 ", *Journal of Alloys and Compounds*, vol. 394, no. 1-2, pp. 292-302, 2005.
 [14] B. Tareev, "Physics of Dielectric Materials", Mir Publishers, Moscow, 1979.
 [15] K. P. Padmasree, D. K. Kanchan, and A. R. Kulkarni, "Impedance and modulus studies of the solid electrolyte system $20\text{CdI}_2\text{-}80[x\text{Ag}_2\text{O-y}(0.7\text{V}_2\text{O}_5\text{-}0.3\text{B}_2\text{O}_3)]$, where $1 \leq x/y \leq 3$ ", *Solid State Ionics*, vol. 177, no. 5-6, pp. 475-482, 2006.
 [16] M. Dong, J. M. Reau, and J. Ravez, "Impedance-spectroscopy analysis of $\text{Ba}_5\text{Li}_2\text{Ti}_2\text{Nb}_8\text{O}_{30}$ ferroelectric ceramics", *Solid State Ionics*, vol. 91, no. 3-4, pp. 183-190, 1996.
 [17] K. S. Rao, D. M. Prasad, P. M. Krishna, B. Tilak, and K. C. Varadarajulu, "Impedance and modulus spectroscopy studies on $\text{Ba}_{0.1}\text{Sr}_{0.81}\text{La}_{0.06}\text{Bi}_2\text{Nb}_2\text{O}_9$ ceramic", *Materials Science and Engineering: B*, vol. 133, no. 1-3, pp. 141-150, 2006.
 [18] P. Ganguly, A. K. Jha, and K. L. Deori, "Complex impedance studies of tungsten-bronze structured

Ba₅SmTi₃Nb₇O₃₀ ferroelectric ceramics”, *Solid State Communications*, vol. 146, no. 11-12, pp. 472-477, 2008.

[19] A. M. Milankovic, V. Licina, S. T. Reis, and D. E. Day, “Electronic relaxation in zinc iron phosphate glasses”, *Journal of Non-Crystalline Solids*, vol. 353, no. 27, pp. 2659-2666, 2007.

[20] S. Saha, and T. P. Sinha, “Low-temperature scaling behavior of BaFe_{0.5}Nb_{0.5}O₃”, *Physics Review B*, vol. 65, pp. 134103 (1-7), 2002.

